BMC Veterinary Research

RESEARCH

Open Access

Intrapatient application of lymphoscintigraphy and near-infrared fluorescence in canine and feline sentinel lymph node mapping and removal

Elisa Maria Gariboldi[1*†], Alessandra Ubiali[1†], Patrizia Boracchi[2], Ester Luconi[3], Roberta Ferrari[1], Luigi Auletta[1], Donatella De Zani[1], Davide Danilo Zani[1], Paola Roccabianca[1], Valeria Grieco[1], Chiara Giudice[1], Camilla Recordati[1] and Damiano Stefanello[1]

Abstract

Background No data regarding near-infrared fluorescence (NIRF) with indocyanine green and its comparison with lymphoscintigraphy are available for sentinel lymph node identification in canine and feline solid malignant tumors. This study compares both techniques in sentinel lymphocentrums mapping and surgical guided sentinel lymph node extirpation.

Results Fifty-four animals with 60 tumors were included, and the combined use of lymphoscintigraphy and NIRF was applied: 80 sentinel lymphocentrums were surgically explored, and 113 sentinel lymph nodes were extirpated. This combination allowed the detection of at least one sentinel lymphocentrum and sentinel lymph node per each tumor. During mapping, the sentinel lymphocentrum detection rate with NIRF was 93%, similar to lymphoscintigraphy with a handheld intraoperative gamma probe (92%). No significant differences among techniques were observed in the surgical guided exploration phase, except that the number of fluorescent sentinel lymph nodes was significantly higher than radioactive ones, and the number of detected metastatic lymph nodes was comparable among the techniques. Surgeons subjectively considered the intraoperative gamma probe more helpful in 46.5% of sentinel lymph node extirpations, NIRF more helpful in 24.2%, and both techniques equally helpful in 29.3% of cases. Overall, they deemed the use of intraoperative gamma probe superior to NIRF for axillary lymphadenectomies and NIRF superior to lymphoscintigraphy for head and neck lymphadenectomies.

Conclusions Despite some differences between the techniques, NIRF with indocyanine green can be considered a practical and viable alternative to lymphoscintigraphy for sentinel lymphocentrum mapping and guided sentinel lymph node removal in small animal oncologic practice, particularly where lymphoscintigraphy is not accessible.

†Elisa Maria Gariboldi and Alessandra Ubiali contributed equally to this work.

*Correspondence:
Elisa Maria Gariboldi
elisamaria.gariboldi@unimi.it

[1]Dipartimento di Medicina Veterinaria e Scienze Animali, Università degli Studi di Milano, Lodi, Italia
[2]Dipartimento di Scienze Biomediche e Cliniche, Università degli Studi di Milano, Milano, Italia
[3]Dipartimento di Scienze Biomediche per la Salute, Università degli Studi di Milano, Milano, Italia

Keywords Dog, Cat, Technetium-99, Indocyanine green, Fluorescence, Lymph node

Background

Sentinel lymph node (SLN) extirpation has been proven to lead to a more accurate staging in canine and feline malignancies [1–4]. Different mapping techniques are reported in veterinary medicine, such as contrast enhanced-ultrasound, radiographic indirect lymphography, indirect computed tomography lymphography, indocyanine based near infrared lymphography, lymphoscintigraphy [5–11]. Most of these are exclusively pre-operative, and therefore need an additional tracer for surgical exploration of the sentinel lymphocentrum (SLC) and SLN extirpation [12, 13].

In humans, lymphoscintigraphy (LPS) is considered the standard care for SLN detection and extirpation [14, 15]. However, law permission, radioactive exposure, and the need for specialized facilities and personnel for radiopharmaceutical management led to the search for alternative techniques. Based on current data published in humans, fluorescence may represent an ideal alternative to radioactive tracers for SLN identification [16–18]. The same concerns exist in small animal practice since LPS for SLN mapping and extirpation is only available in a few facilities. Conversely, although it necessitates specialized equipment, near-infrared fluorescence with indocyanine green (NIRF-ICG) is an emerging technique for SLN mapping and extirpation [3, 12, 13, 19], that does not require legal authorization or dedicated facilities. In addition, fluorescence imaging can be applied in various fields of small animal surgery, including minimally invasive procedures [20–23]. SLN detection rate of NIRF is analogous to LPS in dogs and cats. However, neither technique alone guarantees 100% detection [1, 12, 13, 19, 24]. Combining sentinel lymph node mapping techniques to enhance sentinel lymph node detection is desirable in small animals with solid malignant tumors and has been reported for other preoperative and intraoperative techniques [12, 13]. Although an increase in the SLN detection rate is expected in the case of the combination of LPS and NIRF-ICG, data regarding this are absent in veterinary medicine. Moreover, there is a lack of intra-patient comparison data regarding the performance of these two techniques in SLC mapping and SLN extirpation in dogs and cats.

Based on the latter consideration and the lack of studies focusing on the comparison lymphoscintigraphy and NIRF, the present study aims to compare intra-patient LPS and NIRF-ICG performance in SLC mapping and SLN detection for its removal. Specifically, the purpose is to evaluate the performance and agreement of these two techniques in canine and feline malignant tumors during different phases: (1) the mapping for sentinel lymphocentrum (SLC) identification; (2) the guided surgical exploration of SLC for SLN detection for its removal.

Methods

The characteristics of participants

This observational study was conducted on client-owned dogs and cats with a cytological or histological diagnosis of solid malignant tumors at first presentation, characterized by non-palpable and/or normal-sized regional lymph nodes. These animals were eligible for curative-intent surgery and SLN extirpation and were referred to the Veterinary Teaching Hospital (VTH) of the Università degli Studi di Milano, Lodi, Italy from November 2022 to December 2023. The combined use of LPS and NIRF-ICG was recommended to ensure better identification, detection, and removal of SLC and SLN. Owners signed a written informed consent for all the procedures performed and data collection. This study does not involve animal experimentation, but owned dogs and cats and the methods applied in our study are already widely described and used in small animal clinical practice. All the procedures were performed in accordance with the Italian National legislation for animal welfare (DL 14th March 2014 n.26) and best standard of veterinary practice (Good Veterinary Practice from the Federation Veterinary Europe—Italian National Federation of the Veterinary' Orders [FNOVI] 29th January 2005).

Patients with scars from previous excision of a malignant neoplasm in the absence of lymphadenectomy were also included. Exclusion criteria were: client declined the use of both techniques or SLC surgical exploration, evidence of distant metastases, previous regional lymphadenectomy and neo-adjuvant oncological therapy.

The SLC was defined as the first lymphatic station that included one or more SLNs receiving drainage from the tumor or scar and was expected to be the first site of metastasis. The term "SLC" was used during the mapping phase because LPS and NIRF-ICG are not able to define the individual SLNs within the SLC prior to the intraoperative approach.

Technical information

Complete preoperative staging and curative-intent surgical procedures were conducted according to the current recommendation based on cytological or histological tumor diagnosis [25–27]. Draining lymph nodes were selected and removed based on the combined use of LPS and NIRF-ICG.

Data about patient signalment were recorded: species, breed, sex, age, body weight, body condition score (BCS)

on a nine scale, and number of tumors (single or multiple presentation). The clinical variables of tumors/scars included: anatomical location, dimension, ulceration, the related regional lymphocentrum (RLC) (according to Suami et al. 2013 [28]) and drainage to a single or multiple SLC. Anatomical locations were categorized as limbs (below the elbow/knee, excluding digits), trunk (upper the elbow/knee, included lumbar area, thoracic and abdominal mammary glands), head and neck, inguinal (perineal, genitals, and inguinal mammary glands), digits, and tail regions. Correspondence between identified SLC with RLC was defined as follows: total correspondence if all SLC corresponded with the expected RLC; non-correspondence if all SLC had different locations than the RLC; unpredictable if the RLC could not be determined due to overlap of more than one lymphosome [28, 29]. Skin related to lymphosome, according to Suami's study (2013) [28], was categorized as pigmented or non-pigmented based on clinical appearance.

Data registered were: visualization of radioactive or fluorescent drainage, SLC fluorescence/radioactivity, migration time (in minutes calculated from the injection to the SLC identification), number of SLNs per SLC detected intra-operative by each technique, total number of hot/fluorescent SLNs, presence of residual fluorescence or radioactivity in the SLC after each SLN removal. The time of tumor/scar excision and SLN biopsy (both calculated as time in minutes from skin incision to last skin suture) were also recorded, and any intra-operative and post-operative complication of the lymphadenectomy or tumor excision was registered (if it occurred). Histopathological data collected were: tumor type, histological grade (when applicable), and metastatic status of SLN.

The LPS and NIRF-ICG mapping and intraoperative phase are detailed below and shown in Figs. 1 and 2.

Mapping for SLC identification

Both LPS and NIRF-ICG, were always performed on each animal on the same day of the surgery. These techniques were applied as described in previous studies [2, 3, 10, 11, 19, 24]. The mapping for SLC identification with preoperative planar-LPS was performed as follows: a volume of 0,5 ml of technetium-99 metastable (99mTc) labeled nano-sized human serum albumin (Nanoalbumon; Radiopharmacy Laboratory Ltd, Budaörs, Hungary) with an activity ranged between 23 and 30 MBq was intradermally and subcutaneously injected peritumorally in four sites at a distance of 1 to 2 mm from the gross margins of the tumor by the same operator (DDZ). Planar static images were immediately acquired using a single head gamma camera (Picker Prism 2000XP, Picker International, Highland Heights, Ohio). The average time elapsed between radiotracer injection and completion of planar image acquisition was approximately 12 min. The minimum time required for visualization of SLC uptake was 60 s, while the maximum time observed was 5 min. Following acquisition of planar images adequate for SLC identification, the patient was subsequently transferred to the operating room. Radiopharmaceutical mapping for SLC was then completed with the use of a handheld intraoperative gamma-probe (HIGP - Crystal probe SG04; Crystal Photonic GmbH, Berlin, Germany) connected to a display indicating the radioactive count (RC).

After planar-LPS, fluorescence lymphography was always performed in the operating room immediately before surgery. A volume of 0.2 ml (2.5 mg/ml) of ICG (Verdye, Diagnostic Green, Garrycastle, Ireland) plus 0.2 ml of 0.9% NaCl in a sterile syringe was injected in four quadrants peritumorally or around the scar by the surgeons (DS, RF) and a gentle massage was applied. A NIRF-camera (SPY-Elite Imaging system, Stryker, MIDA

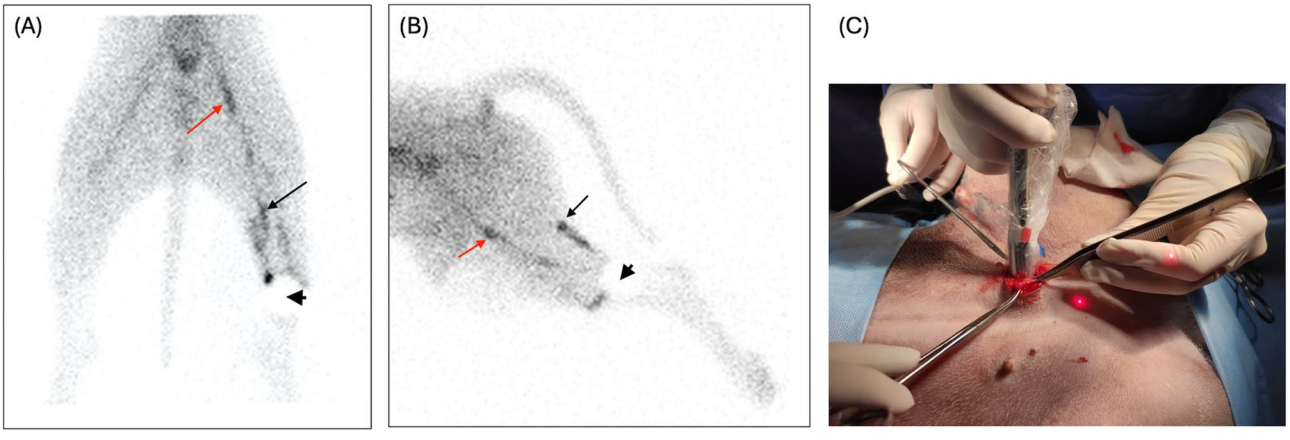

Fig. 1 LPS mapping for SLC identification and guided surgical exploration for SLN detection. Example of a dog with a soft tissue sarcoma on the left lateral hock. (**A**) left lateral and (**B**) dorsal planar static images obtained by preoperative planar-LPS for mapping for SLC identification. Arrowhead: the injection site of Technetium-99 masked with a 2 mm thick lead shield; Black arrow: popliteal SLC; Red arrow: inguinal SLC. (**C**) use of HIGP to complete LPS mapping in the operating room and during guided surgical exploration of inguinal SLC for SLNs detection and for surgical field check after each SLN removal

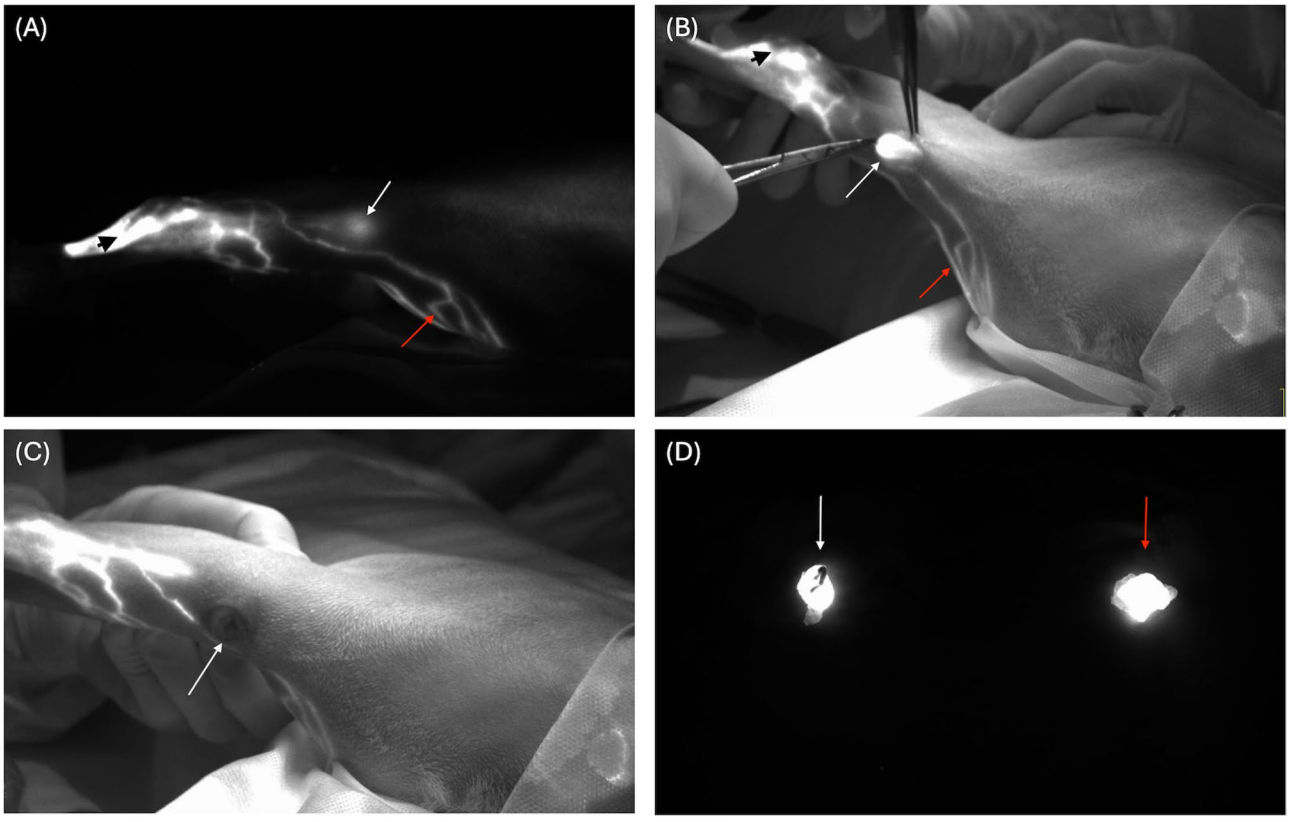

Fig. 2 NIRF-ICG mapping for SLC identification and surgical guided exploration for SLN detection. Example of the same dog with a soft tissue sarcoma on the left lateral hock. Caudal aspect of the hind-limb of the dog placed in right lateral recumbency (**A**) Fluorescence image obtained by NIRF-ICG camera in monochromatic mode for mapping for SLC identification. Arrowhead: the injection site of indocyanine green; White arrow: popliteal SLC; Red arrow: lymphatic network going proximal in inguinal SLC direction. (**B**) SLN fluorescence visualization during surgical exploration of the SLC in the intra-operative phase. (**C**) Post-excision check of the surgical field after the first SLN removal in popliteal region: no others fluorescent nodes are visible within the lymphocentrum (white arrow). (**D**) Fluorescent inguinal (red arrow) and popliteal (white arrow) SLNs removed during ex-vivo evaluation with NIRF-ICG-camera.

Tecnologia medica S.p.A) was positioned 20–30 cm above the surgical field and SLCs were determined by the images of fluorescence lymphography acquired and visualized on the display. Operating lights were turned to endoscopy mode during the explorative phase of the surgery. They were turned off for acquiring images during mapping and detection of surgical approach to the SLC, post-excisional surgical field check, and ex vivo evaluation of SLN.

In the absence of migration, the time of observation with the techniques was extended up to approximately 20–30 min. All lymphocentrums identified by at least one technique were considered SLC and surgically explored. The surgical approach to the SLC was established case by case according to tracers' guidance (maximum RC through the tissue above the SLC for the LPS and direct fluorescence of SLC for NIRF-ICG) and anatomic landmarks [30–33]. If mapping had suggested an intra-abdominal or intrathoracic SLC (e.g., medial iliac or sternal lymphocentrums), a routine celiotomy or thoracotomy would have been performed to visualize the lymphocentrum. Mapping for ICG and 99mTc was considered failed if no drainage or SLC focal uptake was detected by NIRF-camera or by LPS (planar-LPS with HIGP).

When, during mapping, the two techniques identified different SLCs, all of them were checked for both radioactivity and fluorescence. In the presence of simultaneous failures of both techniques, all RLC [28] were checked for both radioactivity and fluorescence. If no radioactivity or fluorescence was detected, the RLC was explored for nodal removal.

All the devices (RC display and imaging system screen showing fluorescence in monochromatic mode) were visible to the surgeons during all the procedures in the operating room. The presence of a "tumor shine-through effect", defined as the overlap of the SLC with tumor/scar radioactivity or fluorescence due to their anatomical proximity, was also recorded.

Guided surgical exploration of SLC for SLN detection

Lymphadenectomy was performed before tumor/scar removal, except when tumor shine-through effect occurred or if SLC was in the same surgical field of

tumor/scar. All procedures were performed by surgeons (DS, RF) with experience in sentinel lymph node extirpation (more than 20 SLN procedures) [34].

All lymph nodes identified by at least one tracer within the SLC were considered SLN and removed and submitted to histopathological analysis. A SLN was considered "hot" when its RC was at least 10% of the RC recorded for the corresponding tumor [11], "fluorescent" when detected by NIRF-camera and confirmed ex vivo by a signal-to-background ratio (SBR) > 1.1 [32]. To avoid the missing of additional SLN within a SLC, after each SLN removal, the surgical field was checked for further residual "hot" and/or fluorescent SLN and if present they were removed. Surgical exploration ended when the radioactive count in the surgical field was less than 10% of the hottest SLN extirpated, and no other fluorescent nodes were visible. The possible presence of ICG leakage in the surgical field from broken lymphatic vessels was also registered. At the end of surgery, radioactivity and fluorescence were evaluated in ex vivo SLNs. In addition, the surgeon subjectively reported after each SLN removal which technique gave the best surgical aid during intraoperative detection and classified in HIGP, NIRF-ICG, or equal performance.

Statistics

Descriptive statistic was used to summarize the distribution of retrieved variables. For variables measured on a numerical scale, the distribution was summarized by the following quantities: minimum, first quartile, median, mean, third quartile, and maximum. For the variables measured on categorical scale the distribution was summarized by absolute frequencies and percentages.

For mapping and SLC identification, LPS (planar-LPS images with HIGP) and NIRF-ICG were compared. The percentage of tumors in which at least a lymphatic tract was detected was reported together with the corresponding 95% confidence interval for each technique (calculated by exact method).

The cases affected by tumor shine-through effect and those in which lymphadenectomy was performed *en bloc* with tumor removal (e.g., superficial inguinal SLN simultaneously removal during regional/unilateral mastectomy) were excluded from mapping comparison.

To evaluate the difference between the SLC detection probability with the two methods, a generalized linear model for the analysis of correlated observations was adopted [35]. Model response (dependent variable) was the binary variable related to the detection of the lymphatic network (coded 1 if detected and 0 if non detected), and the independent variable was the method (included as a binary variable coded 1 if NIRF and 0 for LPS). Model results were reported as prevalence detection ratio (with 95% confidence intervals and *p*-value of Wald Statistics).

The concordance between the two methods was estimated by Bangdiwala's agreement index B (and its 95% confidence intervals), which is appropriate in case of presence of cells with no observations. In this study, the absence of cells occurred when the lymphatic network was not detected using both techniques simultaneously. The index ranges between 0 (no agreement) and 1 (total agreement) [36].

Regarding SLN detection, HIGP and NIRF-ICG guidance were compared to identifying of SLN during SLC surgical exploration. The analysis focused on the percentage of hot and fluorescent extirpated SLNs, and the percentage of residual SLNs detected during post-excision surgical field checks by HIGP and/or NIRF-ICG. The statistical analysis for the comparison of the methods was performed by the previously described approaches.

An explorative analysis of the association between the selected variables and the detection of SLC or SLN for each method was performed for an empirical indirect comparison.

For each variable, the association was evaluated by the Fisher exact test, and the ratio between the percentage of detected SLC (or residual SLN) and the difference between the percentage of detected SLC (or residual SLN) in different categories were reported as measures for the strength of the association. The BCS was categorized as underweight (BCS < 4); normal weight (BCS = 4,5); overweight (BCS > 5). Considering the wide range of pet's body weight, this variable was arbitrarily categorized for statistical purposes into 3 classes: < 9 kg, 9–30 kg, and > 30 kg. For the same reasons, the SLN dimension was categorized into < 10 mm, 10–20 mm, and > 20 mm. The SLC anatomical locations were: head and neck (including parotid, mandibular, and retropharyngeal), superficial cervical, axillary (including axillary and accessory axillary), superficial inguinal, medial iliac, and popliteal [28, 29].

For the ratio and the difference between the percentage of detected SLC (or residual SLN), one of the categories was considered as a "reference" according to the clinical expected better performance of both techniques, for SLC (or residual SLN) detection. The superficial inguinal SLC and SLN anatomical location was considered a reference category among the lymphocentrums identified in this study. According to the lymphosome map [28], the lymphatic territory related to the superficial inguinal SLC borders many other lymphatic territories. This anatomical location increases the likelihood of it being an SLC for malignancies developing in adjacent lymphosomes, making it a possible site frequently involved in mapping and SLN extirpation.

Table 1 Animals' signalment distributed in dogs and cats

	Animals (*n* = 54)
Breed	13 (24.1%) Mixed breed 5 (9.2%) Boxer 3 (5.6%) Golden Retriever 3 (5.6%) Jack Russel Terrier 3 (5.6%) Labrador Retriever 23 (42.5%) Others canine breeds 4 (7.4%) Feline Domestic Shorthair
Age (years)	1.5–13.5
Min - Max	6.5–10.5
1 st Quart-3rd Quart	8.4
Mean	8
Median	
Sex	8 (14.8%)
Female	25 (46.3%)
Spayed Female	15 (27.8%)
Male	6 (11.1%)
Neutered Male	
Bodyweight (kg)	3.4–54.3
Min - Max	9.8–31.8
1 st Quart-3rd Quart	23.2
Mean	22.1
Median	
BCS	0
Underweight	38 (70.4%)
Normal weight	16 (29.6%)
Overweight	

Legend: *BCS* body condition score

An explorative analysis of the association between the above-mentioned variables and the preferred method to detect SLN as surgical aid was performed using the same approach.

All analyses were performed using R Statistical Software (V 4.2.2 R Core Team 2022), packages Geepack [37], epiR [38], irrCAC [39].

Results

Among 67 animals evaluated for surgical purposes during the study period, 13 were excluded because they underwent sentinel lymphadenectomy only guided by one technique (5 cats and 2 dogs underwent only NIRF-ICG, 6 dogs only LPS). A total of 54 animals (50 dogs and 4 cats) were included in the study. Six dogs underwent multiple mapping due to the presence of > 1 tumors and scars (5 dogs had 2 mast cell tumors – MCT, and one dog had 2 mammary gland carcinomas). In the remaining cases the mapping was performed for a single tumor or scar. Overall, both tracers were used for SLC mapping and detection and surgical guided exploration in a total of 60 cases: 46 measurable tumors and 14 scars (4 of which with microscopic disease). Multiple SLCs (range 2–3) were detected in 16 tumors and 1 scar, while only one SLC was detected for each of the remaining 30 tumors and 13 scars. Eighty SLCs (76 peripheral and 4 intra-abdominal) were investigated, and a total of 113 SLNs were removed. Information about animals, tumors/scars, and SLC are summarized in Tables 1, 2 and 3. In 47 (59%) SLC, there was correspondence with the expected RLC; in 18 (22%), there was no correspondence; and in 15 (19%), the RLC was unpredictable.

In 13 tumors and 2 scars (25%), the skin covering the expected lymphosomes was pigmented. Five cases (8%) presented the tumor shine-through effect and in 3 of them the SLCs were *en-bloc* removed in association with

Table 2 Clinical and histopathological features of tumors and scars

	Tumors (*n* = 46)	**Scars (*n* = 14)**
Anatomical location	22	6
Trunk	7	4
Head and neck	10	1
Inguinal/genital	7	3
Limbs		
Maximum dimension	2-100	-
(mm)	9.8–30	
Min - Max	23	
1 st Quart-3rd Quart	20	
Mean		
Median		
Ulceration	5	-
Yes	55	
No		
Histopathological	26 cMCT:	7 cMCT:
diagnosis	4 PG1/KLG	1 PG1/KLG
(*n* = 60)	21 PG2/KLG	6 PG2/KLG
	1 PG3/KHG	2 sMCT
	6 sMCT:	infiltrative
	3 infiltrative	2 lip/oral
	1 circumscribed	melanoma
	2 combined	1 STS
	9 mammary gland carcinomas	1 feline
	1 G II STS	cMCT LG
	1 G II PWT	1 feline
	1 oral fibrosarcoma	mammary
	2 feline cMCT LG	gland
		carcinoma

Legend: *cMCT* cutaneous mast cell tumor, *sMCT* subcutaneous mast cell tumor, *G* grade, *PG* Patnaik grade, *KLG* Kiupel low grade, *KHG* Kiupel high grade, *LG* low grade, *STS* soft tissue sarcoma, *PWT* perivascular wall tumor

Table 3 Sentinel lymphocentrum (SLC) data

	SLC draining measurable tumors (*n* = 65)	**SLC draining scars (*n* = 15)**
SLC anatomical location:	17	2
Axillary (*n* = 19)	3	1
Accessory axillary (*n* = 4)	4	0
Medial iliac (*n* = 4)	20	3
Superficial inguinal (*n* = 23)	3	4
Mandibular (*n* = 7)	2	1
Parotid (*n* = 3)	3	3
Popliteal (*n* = 6)	9	1
Superficial cervical (*n* = 10)	4	0
Retropharyngeal (*n* = 4)		

Legend: *SLC* sentinel lymphocentrum

the tumor, while in the 2 remaining cases the SLC was surgically explored after the tumor excision. In 2 other cases (both tumors on the third mammary gland), the SLC (superficial inguinal) was *en-bloc* excised during unilateral mastectomy even if no tumor shine-through effect was present.

The median surgical times for local tumor or scar removal (including cases where the SLC was in the same surgical field as the tumor) was 40 min (range 7–90 min). The median surgical times for SLC exploration and SLN removal was 21.5 min (range 5–60 min).

The only post-injection complication was peritumoral mild edema noticed in 16/60 (26.7%) cases (all MCT), and it was observed both after ^{99m}Tc and ICG injections. No intra-operative complications were registered. Five post-operative complications (6%) occurred at the SLC surgical site, 1 of them required surgical revision, whereas 13 complications (21.7%) took place at the tumor surgical site, 2 of which required surgical revision.

Mapping for SLC identification

In all the tumors/scars included, the combined use of techniques led to the detection of at least one SLC. In 43 cases (71.7%), at least one tracer migrated to a single SLC, while in 17 cases (28.3%) to multiple SLCs (range: 2–4 SLCs per tumor) as detailed in Table 3. No lymphatic drainage or SLC focal uptake was detected during LPS mapping (planar-LPS with HIGP) in 1/60 case (2%) (one measurable MCT on the head and neck), and with NIRF-ICG mapping in 3/60 cases (5%) (one scar of a mammary gland carcinoma on the trunk and 2 measurable MCT one on the head and neck and one on the trunk). In 5 cases (8.3%) (4 tumors and one scar), the tumor shine-through effect was present with both techniques and in two of these tumors also exhibited lymphatic migration to an another SLC. In 50/60 (83%) tumors/scars the two techniques detected the same SLCs during mapping, in 6/60 (10%) the agreement of the detection was partial and in 4/60 (7%) cases had no agreement. The time of SLC identification ranged from immediate to 12 min for the LPS and from immediate to 10 min for NIRF-ICG.

Table 4 Comparison among LPS and NIRF-ICG in identifying SLC (considered only the 73 SLCs included)

		NIRF-ICG		
		SLC identified	**SLC not identified**	**Total**
Planar-LPS with HIGP	SLC identified	62 (84.93%) 95%C.I.:74.64%–92.23%	5	67 (91.78%) 95%C.I.: 82.96%–96.92%
	SLC not identified	6	-	6 (8.22%)
	Total	68 (93.15%) 95%C.I.: 84.74%–97.74%	5 (6.85%)	73

C.I. confidence interval

Agreement. Bangdiwala's B: 0.838 (95% C.I.: 0.743–0.934)

Comparison between the percentage of identified SLC in the two techniques. Percentage ratio (NIRF-ICG vs. Planar-LPS with HIGP): 1.015 (95%C.I.: 0.925–1.113) $P = 0.754$

A total of 80 SLCs were identified using the combination of the techniques. Seven out of 80 SLCs were excluded because they received an *en-bloc* excision (which precluded the possibility of exploring the surgical approach to the SLC) and/or presented tumor shine-through effect. Among 73 SLCs included in this analysis, the SLC was identified in 67/73 (92%) using preoperative planar-LPS with HIGP, and 68/73 (93%) by NIRF-ICG. Within the 6 cases of LPS mapping failure, in only one SLC a hot SLN was removed. On the other hand, among the 5 NIRF-ICG mapping considered as failed, in 3 SLCs (2 superficial cervical and one superficial inguinal) the network was not visible percutaneously, but the fluorescence of SLC was detected only after or during surgical exploration. In 42/68 NIRF-ICG mapping (62%) lymphatic network and the SLC were directly visible percutaneously. In the remaining 26/68 (38%), only the lymphatic network leading to the SLC was visible. Specifically, 22/26 (83%) were peripheral SLCs and the SLC location was inferred with reasonable accuracy by projecting downward and slightly outward from the point where the lymphatic channel dives deep and disappears from the surgeon's view. In the remaining 4/26 (17%) non peripheric SLCs (all medial iliac SLCs) the fluorescent lymphatic network was visible on the lateral side of the trunk and then went deep, perforating the abdominal wall, and the SLC fluorescence was assessed after celiotomy.

Results of the comparison between preoperative planar-LPS with HIGP and NIRF-ICG mapping are summarized in Table 4. Considering 73 SLCs, both techniques agreed on identifying 62 (84.93%) and disagreed on 11 (15.07%). The strength of agreement, measured using the B index, was 0.838 (Table 4). Planar LPS with HIGP identified 91.78% of SLCs, while NIRF-ICG identified 93.15%; the difference between these percentages was not statistically significant ($P = 0.754$)..

No significant associations were found between mapping with preoperative planar-LPS with HIGP and NIRF-ICG and the variables considered: BCS, SLC location, weight, and skin pigmentation (Table 5).

Guided surgical exploration of SLC for SLN detection

Results of the comparison between HIGP and NIRF-ICG during SLC surgical exploration are summarized in Table 6. In all the included tumors/scars the combined intraoperative use of techniques led to the detection of at least one SLN within SLC. In 58/80 SLCs (72.5%), a single SLN was identified (in 5 SLCs only by NIRF and 5 SLCs only

Table 5 Association between detection of SLC with LPS vs. NIRF-ICG with selected variables

		LPS (planar-LPS with HIGP) SLC Identified (*n* = 67)	**NIRF-ICG SLC Identified (*n* = 68)**
	Total number of SLC per category	Number identified per category (%)	Number identified per category (%)
BCS	52	49 (94.23%)	49 (94.23%)
Normal Weight			
*Overweight	21	18 (85.71%)	19 (90.48%)
		PR = 0.91 C.I. (0.75, 1.10) PD= −8.52 C.I. (−24.77, 7.74) *P* = 0.345	PR = 0.96 C.I. (0.82, 1.12) PD= −3.75 C.I. (−17.82, 10.31) *P* = 0.621
SLC location	19	19 (100.00%)	18 (94.74%)
Axillary	4	4 (100.00%)	4 (100.00%)
Accessory axillary	4	4 (100.00%)	4 (100.00%)
Medial iliac	18	17 (94.44%)	16 (88.89%)
Superficial Inguinal	7	5 (71.43%)	7 (100.00%)
Mandibular	3	3 (100.00%)	3 (100.00%)
Parotid	4	4 (100.00%)	4 (100.00%)
Popliteal	10	9 (90.00%)	8 (80.00%)
Superficial cervical	4	2 (50.00%)	4 (100.00%)
Retropharyngeal			
		P = 0.055	*P* = 0.892
SLC location	18	17 (94.44%)	16 (88.89%)
*Superficial Inguinal	23	23 (100%)	22 (95.65%)
Axillary + Accessory Axillary			
		PR = 0.94 C.I. (0.84, 1.06) PD= −5.56 C.I. (−16.14, 5.03) *P* = 0.439	PR = 0.93 C.I. (0.77, 1.12) PD= −6.76 C.I. (−23.50, 9.98) *P* = 0.573
*Superficial Inguinal	18	17 (94.44%)	16 (88.89%)
Head and neck	14	10 (71.43%)	14 (100.00%)
		PR = 1.32 C.I. (0.93, 1.88) PD = 23.02 C.I. (−2.91, 48.94) *P* = 0.142	PR = 0.89 C.I. (0.75, 1.05) PD= −11.11 C.I. (−25.63, 3.41) *P* = 0.492
* Superficial Inguinal	18	17 (94.44%)	16 (88.89%)
Superficial cervical	10	9 (90.00%)	8 (80.00%)
		PR = 1.05 C.I. (0.83, 1.33) PD = 4.44 (−16.95, 25.84). *P* > 0.99	PR = 1.11 C.I. (0.78, 1.58) PD = 8.89 C.I. (−19.84, 37.62) *P* = 0.601
Weight			
< 9 kg	17	16 (94.12%)	16 (94.12%)
9–29.99 kg	31	27 (87.10%)	29 (93.55%)
>=30 kg	25	24 (96.00%)	23 (92.00%)
		P = 0.557	*P* > 0.99
*>=30 kg	25	24 (96.00%)	23 (92.00%)
< 9 kg	17	16 (94.12%)	16 (94.12%)
		PR = 1.02 C.I. (0.88, 1.18) PD = 1.88 C.I. (−11.69, 15.45) *P* > 0.99	PR = 0.98 C.I. (0.83, 1.15) PD= −2.30 C.I. (−20.75, 13.33) *P* > 0.99
*>=30 kg	25	24 (96.00%)	23(92.00%)
9–29.99 kg	31	27(87.10%)	29(93.55%)
		PR = 1.10 C.I. (0.94, 1.29) PD = 8.90 C.I. (−5.18, 22.98) *P* = 0.367	PR = 0.98 C.I. (0.85, 1.14) PD= −2.12 (−17.55, 13.32). *P* > 0.99
Skin pigmentation			

Table 5 (continued)

		LPS (planar-LPS with HIGP) SLC Identified ($n=67$)	NIRF-ICG SLC Identified ($n=68$)
*No	59	54 (91.53%)	56 (94.92%)
Yes	14	13 (92.86%)	12 (85.71%)
		PR = 0.99 C.I. (0.84, 1.16)	PR = 1.11 C.I. (0.89, 1.38)
		PD=−1.33 C.I. (−16.58, 13.92)	PD = 9.20 C.I. (−9.97, 28.37)
		$P>0.99$	$P=0.242$

Legend: *PR* percentage ratio, *PD* percentage difference, *Pp*-value of Fisher exact test, *C.I.* 95% confidence interval,

PR: the number of SLCs identified in 100 SLCs of the reference category is PR times the number of SLCs identified in 100 SLCs of the other category

PD: per 100 SLCs in the reference category, PD is the number of SLCs identified in excess (or reduction) compared to 100 SLCs in the other category

*reference category (numerator in PR and first term in the PD)

Table 6 HIGP and NIRF-ICG in identifying SLN during surgical exploration

		NIRF-ICG		
		Fluorescent SLN	Non-fluorescent SLN	Total
HIGP	Hot SLN	96 (84.96%) 95%C.I.: 77.01%- 90.99%	4	100 (88.50%) 95%C.I.: 81.13%-93.73%
	Non-hot SLN	13	-	13 (11.50%)
	Total	109 (96.46%) 95%C.I.: 91.18%–99.03%	4 (3.54%)	113

C.I. confidence interval

Agreement. Bangdiwala's B: 0.841 (95% C.I.: 0.768–0.915)

Comparison between the percentage of identified SLN in the two techniques. Percentage ratio (NIRF-ICG vs. Planar-LPS with HIGP): 1.09 (95% C.I.: 1.011–1.175) $P=0.025$

by HIGP) while 22/80 SLCs (27.5%) presented multiple SLNs (range, 2–4) and only one case was positive only by NIRF. A total of 113 SLNs were extirpated: 96/113 SLNs (85.0%) were both fluorescent and hot; 13/113 SLNs (11.5%) were fluorescent but non-hot; 4/113 SLNs (3.5%) were hot but non-fluorescent. The percentage of excised fluorescent nodes was significantly higher than that of hot nodes (percentage ratio = 1.09, $P=0.025$). The agreement calculated with the B index was 0.841. (Table 6)

At histopathological analysis, 42/113 SLNs (37.2%) were metastatic (41 SLNs were metastatic from mast cell tumors and one from mammary gland carcinoma). Among the 6 SLCs that during mapping were identified exclusively by NIRF-ICG, 2 SLCs contained at least one metastatic SLN; among the 5 SLCs identified exclusively by planar lymphoscintigraphy with HIGP, 3 contained at least one metastatic lymph node. Details about SLN metastatic status and the presence of fluorescence and radioactivity are reported in Table 7.

A comparison of the techniques related to the guided surgical exploration was possible performed in 99/113 SLNs (87.6%). The remaining 14 nodes (from 5 SLCs) were removed *en-bloc* with the tumor due to their anatomical proximity, making guided surgical exploration not possible. Therefore, these nodes were excluded from the surgical exploration comparison, but the fluorescence and radioactivity of each SLN were evaluated ex vivo.

A total of 99 surgical fields were checked after the SLNs removal. The detection of a residual SLN was reported in 26/99 surgical fields (26.3%): in 18/26 of them (69.2%) the residual SLN was identified by both techniques, in 5/26 (19.2%) by NIRF-ICG only, and in 3/26 (11.6%) by HIGP only. All residual lymph nodes were always removed and underwent to histopathological analysis.

No statistically significant difference was found between HIGP and NIRF-ICG in the detection rate of a residual SLN during SLC exploration after the first SLN removal (percentage ratio = 1.10; $P=0.733$). The concordance of the techniques in the post-excision check was 91.92%. The agreement calculated with the B index was 0.882. Details of post-excisional checks in both techniques are reported in Table 8.

The association between the investigated variables and the detection of a residual SLN by HIGP and NIRF-ICG during SLC surgical exploration is reported in Table 9. No significant associations were found in this analysis for HIGP surgical exploration. Considering the NIRF-ICG surgical field check, a significant association was found only with SLC anatomical location ($P=0.004$). Regarding SLC anatomical location, NIRF-ICG during guided surgical exploration identified more superficial inguinal residual SLN than axillary or accessory axillary residual

Table 7 Metastatic status of SLNs and presence of fluorescence, radioactivity

	Fluorescent – Hot	Fluorescent – Non-hot	Hot – Non-fluorescent	Non-hot – Non-fluorescent	Total
Metastatic	37	3	2	0	42
Non-metastatic	59	10	2	0	71
Total	96	13	4	0	113

Table 8 HIGP and NIRF-ICG in identifying residual SLN during surgical exploration

		NIRF-ICG		
		Identified residual SLN	**Not identified residual SLN**	**Total**
HIGP	Identified residual SLN	18 (18.18%) 95% C.I. 11.41%- 27.48%	3	21 (21.21%) 95%C.I. 13.89%–30.81%
	Not identified residual SLN	5	73(73.74%) C.I. 63.76%-81.84%	78
	Total	23 (23.23%) 95%C.I. 15.58%–33.00%	76	99

C.I. confidence interval

General Concordance 91/99 = 91.92% (95% C.I. 84.24% – 96.19%). Agreement. Bangdiwala's B: 0.882 (95% C.I.: 0.801–0.963)

Comparison between the percentage of identified SLN in the two techniques. Percentage ratio (NIRF-ICG vs. Planar-LPS with HIGP): 1.10 (95% C.I.: 0.650–1.846) $P = 0.733$

SLN ($P = 0.024$). The percentage of residual SLN identified in the superficial inguinal SLC was 26.77 higher than in axillary or accessory axillary SLC, and the percentage of identified superficial inguinal residual SLN was 7.79 times compared to those in axillary or accessory axillary.

The residual fluorescence caused by leakage of ICG after rupture of lymphatic vessels was recorded in 24/99 cases (24.2%).

During SLC surgical exploration, surgeons subjectively reported HIGP as more helpful in SLN detection and removal in 46 out of 99 cases (46.5%), NIRF-ICG in 24 out of 99 cases (24.2%), and both equally helpful in 29 out of 99 cases (29.3%). Considering the 70 cases where surgeons preferred only one of the two techniques, NIRF-ICG was preferred in 24/70 (34.29%) and HIGP in 46/70 cases (65.71%). Out of 24 cases of fluorescence leakage, NIRF and HIGP were equally helpful in 6 cases (25%) during SLC surgical exploration. In the remaining 18 cases, HIGP was more helpful in 13/24 cases (72.2%), while NIRF was more helpful in 5/24 cases (27.8%).

The association between the preferred technique and all the checked variables for these 70 cases is summarized in Table 10. The results of the association highlight that only the anatomical location of the SLC showed a significant association ($P < 0.01$). Regarding the comparison between superficial inguinal and axillary + accessory axillary nodes ($P = 0.054$), NIRF-ICG was reported as the best tool for the removal of superficial inguinal nodes (7/23 = 30.43% vs. 1/19 = 5.25%, PR = 5.78), while HIGP was reported as the best tool for the removal of axillary + accessory axillary nodes (16/23 = 69.57% vs. 18/19 = 94.74%, PR = 0.73). About the comparison between superficial inguinal and head and neck nodes ($P < 0.001$), NIRF-ICG was reported as the best tool for the removal of head and neck nodes (7/23 = 30.4% vs. 13/15 = 86.67%, PR = 0.35), while HIGP was reported as the best tool for the removal of superficial inguinal nodes (6/23 = 26.09% vs. 2/15 = 13.33%, PR = 1.96). Medial iliac and popliteal lymphocentrum (and related SLNs) were excluded from the analysis with the reference categories (superficial inguinal) due to low numerosity (< 10).

Discussion

The present study compared the two techniques using oncological cases that spontaneously presented at our VTH during the study period. The advantage of this study is that it is conducted in a daily clinical practice situation, mimicking the performance of the techniques used to identify SLC and SLN and related surgical guided removal. To better represent daily clinical practice in a referral small animal veterinary oncologic centre, the study encompassed various tumor types, measurable macroscopic diseases or scars, and included both canine and feline species, drawing on recently published data [2–4, 19, 24, 40].

The results of the present study confirm the high detection rate of SLC mapping for both techniques, as previously reported in the literature [2, 19], and, when used in combination, the detection rare of SLB may further increase. In fact, the combined use of NIRF-ICG and LPS identifying at least one SLC and the detection and removal of at least one SLN for each tumor leading to a 100% detection rate. Conversely, while the combined use may provide complementary diagnostic benefits, the increased cost could represent the major limitation for the owners. The techniques were compared at two time points: mapping for SLC identification and guided surgical exploration of SLC for SLN detection. No statistical differences were found during SLC mapping between LPS and NIRF-ICG, and their detection rate was similar (respectively 92% and 93%). Despite the well-known ability of fluorescence to allow the surgeon to visualize lymphatic flow and SLCs through the skin in real-time [41], its recognized limit is the low visualization of deeper lymphatic networks and SLCs. Nevertheless, the absence of visualization of fluorescent lymphatic flow was observed in our study only in 5 SLCs, and in 3 of them, SLC fluorescence was detected during the surgical exploration phase. This indicates that, in these 3 cases, ICG reached the nodes, but lymphatic flows were too deep to be detected by the surgeons during the mapping phase before the surgical exploration. Albeit a few cases of tumors with a SLN medial iliac migration ($n = 4$), it should be noted that the two techniques had the same performance. Despite the depth of the SLC, the fluorescent flow was visible on the lateral side of the trunk

Table 9 Association between detection of a residual SLN by HIGP and NIRF-ICG with selected variables

	Total number of SLN for category	Residual SLN identified by HIGP (*n* = 21/26)	Residual SLN identified by NIRF-ICG (*n* = 23/26)
BCS			
Normal Weight	69	15 (21.74%)	15 (21.74%)
*Overweight	30	6 (20.00%)	8 (26.67%)
		PR = 0.92 (C.I. 0.40, 2.14) PD= −1.74 (C.I. −19.05, 15.57) *P* > 0.99	PR = 1.23 (C.I.0.58, 2.58) PD = 4.93 (C.I.−13.65, 23.51) *P* = 0.612
SLN location			
Axillary	21	2 (9.52%)	0 (0.00%)
Accessory axillary	4	1 (25%)	1 (25%)
Medial iliac	7	3 (42.9%)	3 (42,9%)
Superficial Inguinal	26	6 (23.1%)	8 (30.8%)
Mandibular	11	2 (18.2%)	4 (36.4%)
Parotid	8	5 (62.5%)	5 (62.5%)
Popliteal	7	1 (14.3%)	1 (14.3%)
Superficial cervical	11	1 (9.09%)	1 (9.09%)
Retropharyngeal	4	0 (0.00%)	0 (0.00%)
		P = 0.09	*P* = 0.004
SLN location			
*Superficial inguinal	26	6 (23.08%)	8 (30.77%)
Axillary + accessory Axillary	25	3 (12.00%)	1 (4.00%)
		PR = 1.92 (C.I. 0.54, 6.87) PD = 11.08 (−9.53, 31.68) *P* = 0.465	PR = 7.69 (C.I.1.04, 57.13) PD = 26.77 (C.I.7.44, 46.10) *P* = 0.024
*Superficial Inguinal	26	6 (23.08%)	8 (30.77%)
Head and neck	23	7 (30.43%)	9 (39.13%)
		PR = 0.76 (C.I. 0.30, 1.93) PD= −7.36 (−32.17, 17.46) *P* = 0.747	PR = 0.79 (C.I. 0.36, 1.70) PD=−8.36(C.I.−35.05, 18.33) *P* = 0.564
*Superficial Inguinal	26	6 (23.08%)	8 (30.77%)
Superficial cervical	11	1 (9.09%)	1 (9.09%)
		PR = 2.54 (0.34, 18.69) PD = 13.99 (−9.49, 37.46) *P* = 0.649	PR = 3.38 (C.I. 0.48, 23.92) PD = 21.68 (C.I.−2.88, 46.24) *P* = 0.229
Weight			
< 9 kg	25	6 (24.00%)	8 (32.00%)
9–29.99 kg	40	7 (17.50%)	7 (17.50%)
>=30 kg	34	8 (23.53%)	8 (23.53%)
		P = 0.7433	*P* = 0.3874
*>=30 kg	34	8 (23.53%)	8 (23.53%)
< 9 kg	25	6 (24.00%)	8 (32.00%)
		PR = 0.98 (C.I. 0.39, 2.47) RD= −0.47 (C.I. −22.46, 21.52) *P* > 0.99	PR = 0.74 (C.I. 0.32, 1.69) PD=−8.47(C.I.−31.66, 14.72) *P* = 0.559
*>=30 kg	34	8 (23.53%)	8 (23.53%)
9–29.99 kg	40	7 (17.50%)	7 (17.50%)
		PR = 1.34 (C.I.0.54, 3.33) PD = 6.03 (C.I.−12.46, 24.52) *P* = 0.572	PR = 1.34 (C.I.0.54, 3.33) PD = 6.03 (−12.46, 24.52) *P* = 0.572

Legend: *PR* percentage ratio, *PD* percentage difference, *Pp*-value of Fisher exact test, *C.I.*: 95% confidence interval

*reference category: the numerator in PR and the first term in PD; Head and neck: mandibular + parotid + retropharyngeal

PR: the number of SLNs identified in 100 SLNs of the reference category is PR times the number of SLNs identified in 100 SLNs of the other category

PD: per 100 SLNs in the reference category, PD is the number of SLNs identified in excess (or reduction) compared to 100 SLNs in the other category

and then went deep, perforating the abdominal wall as described in previous anatomical studies [42, 43].

The comparison among techniques during the surgical exploration phase showed that excised SLN were significantly more frequently fluorescent than hot: this result follows with previous human and veterinary literature [12, 44, 45]. The hypothesized explanation is that the nanocolloidal formulation of 99mTc increases the

Table 10 Association between surgical aid offered by HIGP and NIRF-ICG in SLN identification and investigated variables.

	Number per category (99 SLN)	Number preferred one of NIRF-ICG or HIGP (70 SLN)	Number NIRF-ICG preferred (%) 24 SLN (34.29%)
BCS			
Normal weight	69	46	17 (36.96%)
*Overweight	30	24	5 (20.83%)
			PR = 0.56 C.I. (0.24, 1.34) PD= −16.12 (−37.54, 5.29) *P* = 0.189
SLN location			
Axillary	21	18	0 (0.00%)
Accessory axillary	4	1	1 (100.00%)
Medial iliac	7	1	1 (100.00%)
Superficial inguinal	26	23	7 (30.43%)
Mandibular	11	7	7 (100.00%)
Parotid	8	6	4 (66.67%)
Popliteal	7	4	1 (25.00%)
Superficial cervical	11	8	1 (12.50%)
Retropharyngeal	4	2	2 (100.00%)
			P < 0.001
*Inguinal	26	23	7 (30.43%)
Axillary + accessory axillary	25	19	1(5.26%)
			PR = 5.78 (C.I. 0.78, 42.95) PD = 25.17 (3.85, 46.49) *P* = 0.054
*Superficial Inguinal	26	23	7 (30.43%)
Head and neck	23	15	13 (86.67%)
			PR = 0.35 (C.I. 0.18, 0.67) PD= −56.23 (C.I.−81.72, −30.75) *P* < 0.001
*Superficial Inguinal	26	23	7 (30.43%)
Superficial cervical	11	8	1 (12.50%)
			PR = 2.43 (C.I. 0.35, 16.85) PD = 17.93 (C.I. −11.71, 47.58) *P* = 0.642
Weight			
< 9 kg	25	21	10 (47.62%)
9–29.99 kg	25	20	7 (35.00%)
>=30 kg	34	29	7 (24.14%)
			P = 0.2306
*>=30 kg	34	29	7 (24.14%)
< 9 kg	25	21	10 (47.62%)
			PR = 0.51 (C.I. 0.23, 1.11) PD= −23.48 (C.I. −49.92, 2.95) *P* = 0.131
*>=30 Kg	34	29	7 (24.14%)
9-29.99 Kg	25	20	7 (35.00%)
			PR = 0.69 (C.I.0.29, 1.66) PD= −10.86 (C.I. −36.93, 15.21) *P* = 0.524
SLN size (mm)			
< 10	24	16	7 (43.75%)
10–20	51	35	11(31.43%)
> 20	24	19	6 (31.58%)
			P = 0.6811
*>20	24	19	6 (31.58%)
< 10	24	16	7 (43.75%)

Table 10 (continued)

	Number per category (99 SLN)	Number preferred one of NIRF-ICG or HIGP (70 SLN)	Number NIRF-ICG preferred (%) 24 SLN (34.29%)
			PR = 0.72 (C.I. 0.30, 1.71) PD= −12.17 (C.I.−44.23, 19.89) *P* = 0.503
*>20	24	19	6 (31.58%)
10–20	51	35	11 (31.43%)
			PR = 1.00 (C.I. 0.44, 2.29) PD = 0.15 (C.I. −25.80, 26.10) *P* > 0.99

tracer nodal retention, while low molecular weight of ICG allows a rapid transit through lymphatic vessels and short nodal retention [44]. The combined use of these two guiding techniques and the two tracers (99mTc and ICG) increases the number of extirped nodes and may maximize the chance of detecting nodal metastases [45]. Nevertheless, despite the higher number of fluorescent SLNs extirpated, the number of metastatic SLNs is comparable in the two techniques (Table 7), suggesting that fluorescence was associated with removal of an adjunctive number of SLNs. Therefore, the extirpation of a higher number of nodes seems not to produce an upper tumor stage migration as previously reported in human and veterinary literature [12, 45].

Based on results of this study it is not possible to determine whether the additional lymph nodes removed can be considered or not second-tier nodes. Considering that in human oncology the specific definition and location of second tier lymph nodes can vary depending on the type of cancer and the anatomical region involved [46], at this moment the authors do not have such indications to correctly define the first and second tier in dogs. Further studies should focus on this aspect of advanced imaging techniques to better define the functional role of these nodes and to potentially adapt the human-derived staging system for veterinary use [47].

However, during SLC surgical exploration NIRF-ICG and LPS with HIGP performed similarly when checking the surgical field after the first SLN removal. The concordance of the two techniques, indeed, increased during the SLN removal phase. These results also underline that NIRF-ICG and HIGP guidance showed a greater advantage in the intraoperative phase by ensuring better extirpation of all SLNs linked to the tumor within an SLC [11, 48].

As a part of the study, we also explored the opinions of the surgeons about the surgical aid provided by each technique in SLN extirpation. According to the surgeons, HIGP was considered the best tool in 46.5% while ICG in 24.2% of cases. It should be also noted that the surgical aid of both techniques was associated with the SLC anatomical location (Table 10). Indeed, HIGP and NIRF-ICG seem to offer different kinds of help. NIRF-ICG was considered the best tool during head and neck (parotid, retropharyngeal, and mandibular) SLC detection, probably due to the close proximity of the tumor/scar with most SLC that could increase the risk of tumor radioactive shine-through effects as previously reported in human literature [49]. Conversely, the use of HIGP was regarded as the best surgical aid mostly in axillary SLCs, according to the surgeons' opinions. A possible explanation could be due to the easy handling and high sensitivity of the probe: the probe can be inserted into the surgical field and can reach the deepest SLNs even in a small deep surgical field such as the axillary region. On the contrary, the type of NIRF-camera used for this study was placed above the surgical field, not directly handheld by the surgeon. Indeed, the visualization of the fluorescence was related to the anatomical conformation, laser angulation, and depth of the SLN. It is unknown to the authors if the use of a different NIRF-camera could improve their performance in this SLC location; however, it should be pointed out that recent research suggests a different approach for axillary SLC, using a minimally invasive endoscopic technique. This technique might be further refined with the addition of ICG [50].

Additionally, considering the surgeons' opinions, the use of HIGP was deemed more comfortable compared to NIRF-ICG in most of cases of fluorescence leakage. Indeed, the leakage of ICG, observed in 24 surgical fields, could produce fluorescent contamination of the surgical field, leading to unclear interpretations during the decision-making process in SLC exploration and SLN extirpation. Even if fluorescent imaging interpretation has a quick learning-curve [51], HIGP probably ensures a more objective assessment of residual SLNs in the surgical field, especially for a surgeon at an early stage of the learning curve.

In human medicine, these techniques have mostly been compared for specific tumors in specific anatomical regions, such as breast cancer and head and neck tumors [17, 45, 49]. Our results cannot be equated with those mostly described for humans because we included different canine and feline solid malignant tumors with

various anatomical locations. Conversely, our results could be compared with a study by Stoffels et al. (2015) [14] on human cutaneous melanoma. In that study, the presence of cutaneous melanoma in various anatomical locations and, consequently, SLCs, showed that the use of NIRF-ICG could not replace the standard care use of LPS due to the lower detection rate and the consequent risk of missing most SLNs [14]. Although we investigated different anatomical locations, in our study, the detection rate of NIRF-ICG in mapping and its concordance with LPS were significantly higher compared to the human melanoma study, resembling findings in other canine and feline NIRF-ICG studies [3, 12, 13, 19]. It could be assumed that even in the presence of different anatomical locations, fluorescence is more successful in dogs and cats rather than in humans. This difference between our results and the study of Stoffels et al. (2015) [14], could be related to the obviously different anatomical conformation of humans and pets. Moreover, in humans, it is reported the worst performance of NIRF-ICG in obese patients, in whom fluorescence is visible only after skin incision [14, 52, 53]. On the contrary, in our study, NIRF-ICG did not show an association with BCS or the body weight of the included animals (Tables 5 and 9, and 10). According to the results in our sample population, it seems that, unlike in humans where obesity plays a role in the fluorescence visualization [14, 52, 53], in dogs and cats NIRF-ICG does not depend on BCS or body weight.

In contrast to human medicine, no comparative studies between LPS and NIRF-ICG are available in veterinary medicine regarding SLN mapping and extirpation. Despite LPS being considered the gold standard for SLN detection in humans, its role as a reference standard in dogs and cats has not been established. Based on this consideration, in our study, it was not possible to compare a technique with a gold standard [14, 15]. Therefore, we evaluated the intra-patient performance and agreement between LPS and NIRF-ICG in SLN detection using the described statistical analysis.

The main limitation of this study is the low precision of the estimates, which is one of the consequences of the sample size. It was of interest to compare the association pattern for the pair of techniques to identify SLC and SLN. Although the appropriate method is a regression model, including the two techniques as independent variables and the selected variables as dependent variables, it was impossible to analyze data by this model because of the small sample size and the low number of non-detected SLC and SLN. Moreover, since no information was available regarding a reference standard technique in veterinary medicine, we could not calculate the sample size for adequate statistical power to compare the techniques for identifying SLC and SLN and to obtain a pre-planned precision of the estimates for the concordance index. For this reason, all statistical analyses were performed only for exploratory purposes, and results of the statistical tests should be considered as a measure of "possible evidence" to be confirmed in studies with greater sample size.

Secondly, the study included a few endocavitary lymphocentrums, represented solely by medial iliac SLN, with no cases involving intrathoracic nodes; thus, no assumptions can be made regarding intrathoracic nodes. Furthermore, we enrolled predominantly cutaneous and subcutaneous tumors, precluding assumptions related to tumors in other locations (e.g., oral cavity or anal sac tumors). These limitations are beyond our control, as they depend on clinical referrals to the VTH during the study period.

In the intraoperative phase, the SLN detection and guided removal were similar. Even if NIRF-ICG selected more nodes than HIGP, the tumor staging did not change. Based on this phenomenon, future studies could explore if the additional non-hot but fluorescent nodes may represent second-tier nodes.

In this study, we did not standardize a maximum mapping time for SLN identification. The use of tracers such as technetium and indocyanine green allows real-time tracking of tracer migration from the tumor to the SLC, unlike radiological tracers (e.g., lipiodol, iohexol) that require radiographs or CT scans at predefined intervals to assess migration and cannot be evaluated intraoperatively [6, 7, 54]. As the mapping time can be influenced by multiple factors beyond the tracer's physicochemical properties and/or half-life of the tracer, we believe that a dedicated study on this aspect would be particularly valuable, especially in clinical settings with metastatic or enlarged lymph nodes [55].

Conclusion

In conclusion, despite some peculiar differences for each technique and the confirmed higher performance if combined, NIRF-ICG and LPS showed comparable performance in SLC mapping and SLN extirpation in canine and feline solid malignant tumors based on our results. Although more data on endocavitary nodes (abdominal and thoracic) should be collected, fluorescence can be considered a viable alternative to radiopharmaceuticals in daily clinical practice, particularly when the latter results not accessible. Finally, the results of this study could provide the opportunity to use the performance, and concordance estimates to plan a future study aimed at statistical inference.

Abbreviations

LPS lymphoscintigraphy
NIRF Near-infrared fluorescence
ICG Indocyanine Green
HIGP Handheld Intraoperative Gamma Probe

SLC Sentinel Lymphocentrum
SLN Sentinel Lymph Node
RLC Regional Lymphocentrum
BCS Body Condition Score

Acknowledgements
This work was supported by Università degli Studi di Milano "piano di Sostegno alla Ricerca (linea2) - Progetto DIVAS CORE.

Authors' contributions
Conception and design: E.M.G.; D.S.; A.U.; Data curation: E.M.G.; Investigation: E.M.G.; D.S.; A.U.; R.F.; L.A.; D.DZ.; D, D.Z; P.R.; C.G; V.G; C.R; Methodology: P.B; E.L.; Drafting the paper: E.M.G.; D.S.; Revising it critically for intellectual content: A.U.; R.F.; L.A.; D.DZ.; D, D.Z; P.B; E.L.; P.R.; C.G; V.G; C.R. All authors reviewed the manuscript.

Funding
The cost of ICG for this study was supported by authors' Department (Dipartimento di Medicina Veterinaria e Scienze Animali - Università degli Studi di Milano (DIVAS)) under Grant Linea 2 (PSR2021_DIP_035_DISTEF) (2021, assigned 2022).

Data availability
Raw data are available from the corresponding author upon reasonable request.

Declarations

Ethics approval and consent to participate
Authors declare that ethics approval was not needed for this study. The study does not involve animal experimentation, but owned dogs and cats with spontaneous neoplastic disease and the methods applied in our study are already widely described and used in small animal clinical practice. Owned dogs and cats were referred to Veterinary Teaching Hospital of authors' Departement and underwent standard procedures for curative intent treatments. Before clinical, diagnostic or treatment procedures, all owners provided to sign a written informed consent for all procedures and data collection. All procedures adhered to Italian national legislation for animal welfare (DL 14th March 2014, n. 26) and the best standards of veterinary practice (Good Veterinary Practice, Federation of European Veterinary Associations—Italian National Federation of the Veterinary Orders [FNOVI], 29th January 2005).

Consent for publication
Not applicable.

Competing interests
The authors declare no competing interests.\

Received: 27 January 2025 / Accepted: 20 August 2025
Published online: 09 October 2025

References

1. Worley DR. Incorporation of sentinel lymph node mapping in dogs with mast cell tumours: 20 consecutive procedures. Vet Comp Oncol. 2014;12:215–26. https://doi.org/10.1111/j.1476-5829.2012.00354.x.
2. Chiti LE, Stefanello D, Manfredi M, Zani DD, De Zani D, Boracchi P, et al. To map or not to map the cN0 neck: impact of Sentinel lymph node biopsy in canine head and neck tumours. Vet Comp Oncol. 2021;19:661–70. https://doi.org/10.1111/vco.12697.
3. Chiti LE, Gariboldi EM, Stefanello D, De Zani D, Grieco V, Nolff MC. Sentinel lymph node mapping and biopsy in cats with solid malignancies: an explorative study. Animals. 2022. https://doi.org/10.3390/ani12223116.
4. Arz R, Seehusen F, Meier VS, Nolff MC. Indocyanine-based near-infrared lymphography for real-time detection of lymphatics in a Cat with multiple mast cell tumours. J Feline Med Surg Open Rep. 2022. https://doi.org/10.1177/20551169221074961.
5. Fournier Q, Thierry F, Longo M, Malbon A, Cazzini P, Bisson J, et al. Contrast-enhanced ultrasound for sentinel lymph node mapping in the routine staging of canine mast cell tumours: a feasibility study. Vet Comp Oncol. 2021;19:451–62. https://doi.org/10.1111/vco.12647.
6. Annoni M, Borgonovo S, Aralla M. Sentinel lymph node mapping in canine mast cell tumours using a preoperative radiographic indirect lymphography: technique description and results in 138 cases. Vet Comp Oncol. 2023;21:469–81. https://doi.org/10.1111/vco.12906.
7. Randall EK, Jones MD, Kraft SL, Worley DR. The development of an indirect computed tomography lymphography protocol for sentinel lymph node detection in head and neck cancer and comparison to other sentinel lymph node mapping techniques. Vet Comp Oncol. 2020;18:634–44. https://doi.org/10.1111/vco.12585.
8. Lapsley J, Hayes GM, Janvier V, Newman AW, Peters-Kennedy J, Balkman C, et al. Influence of locoregional lymph node aspiration cytology vs sentinel lymph node mapping and biopsy on disease stage assignment in dogs with integumentary mast cell tumors. Vet Surg. 2021;50:133–41. https://doi.org/10.1111/vsu.13537.
9. Grimes JA, Secrest SA, Northrup NC, Saba CF, Schmiedt CW. Indirect computed tomography lymphangiography with aqueous contrast for evaluation of sentinel lymph nodes in dogs with tumors of the head. Vet Radiol Ultrasound. 2017;58:559–64. https://doi.org/10.1111/vru.12514.
10. Manfredi M, De Zani D, Chiti LE, Ferrari R, Stefanello D, Giudice C, et al. Preoperative planar lymphoscintigraphy allows for sentinel lymph node detection in 51 dogs improving staging accuracy: feasibility and pitfalls. Vet Radiol Ultrasound. 2021;62:602–9. https://doi.org/10.1111/vru.12995.
11. Gariboldi EM, Ubiali A, Chiti LE, Ferrari R, De Zani D, Zani DD, et al. Evaluation of surgical aid of methylene blue in addition to intraoperative gamma probe for sentinel lymph node extirpation in 116 canine mast cell tumors (2017–2022). Animals. 2023. https://doi.org/10.3390/ani13111854.
12. Wan J, Oblak ML, Ram A, Singh A, Nykamp S. Determining agreement between preoperative computed tomography lymphography and indocyanine green near infrared fluorescence intraoperative imaging for sentinel lymph node mapping in dogs with oral tumours. Vet Comp Oncol. 2021;19:295–303. https://doi.org/10.1111/vco.12675.
13. Alvarez-Sanchez A, Townsend KL, Newsom L, Milovancev M, Gorman E, Russell DS. Comparison of indirect computed tomographic lymphography and near-infrared fluorescence sentinel lymph node mapping for integumentary canine mast cell tumors. Vet Surg. 2023;52:416–27. https://doi.org/10.1111/vsu.13929.
14. Stoffels I, Dissemond J, Pöppel T, Schadendorf D, Klode J. Intraoperative fluorescence imaging for sentinel lymph node detection: prospective clinical trial to compare the usefulness of indocyanine green vs technetium Tc 99m for identification of sentinel lymph nodes. JAMA Surg. 2015;150:617–23. https://doi.org/10.1001/jamasurg.2014.3502.
15. Somashekhar SP, Kumar CR, Ashwin KR, Zaveri SS, Jampani A, Ramya Y, et al. Can Low-cost Indo cyanine green florescence technique for Sentinel lymph node biopsy replace dual dye (Radio-colloid and blue dye) technique in early breast cancer: A prospective Two-arm comparative study. Clin Breast Cancer. 2020;20:e576–83. https://doi.org/10.1016/j.clbc.2020.03.013.
16. Kedrzycki MS, Leiloglou M, Ashrafian H, Jiwa N, Thiruchelvam PTR, Elson DS, et al. Meta-analysis comparing fluorescence imaging with radioisotope and blue dye-guided sentinel node identification for breast cancer surgery. Ann Surg Oncol. 2021. https://doi.org/10.1245/s10434-020-09288-7.
17. Bargon CA, Huibers A, Young-Afat DA, Jansen BAM, Borel-Rinkes IHM, Lavalaye J, et al. Sentinel lymph node mapping in breast cancer patients through fluorescent imaging using indocyanine green the influence trial. Ann Surg. 2022;276:913–20. https://doi.org/10.1097/SLA.0000000000005633.
18. Da Silva Sá R, Von Ah Rodrigues RF, Bugalho LA, Da Silva SU, Pinto Nazário AC. Evaluation of the efficacy of using indocyanine green associated with fluorescence in sentinel lymph node biopsy. PLoS One. 2023. https://doi.org/10.1371/journal.pone.0273886.
19. Beer P, Rohrer-Bley C, Nolff MC. Near-infrared fluorescent image-guided lymph node dissection compared with locoregional lymphadenectomies in dogs with mast cell tumours. J Small Anim Pract. 2022;63:670–8. https://doi.org/10.1111/jsap.13529.
20. Korpita MF, Mayhew PD, Steffey MA, Balsa IM, Giuffrida MA, Chohan AS, et al. Thoracoscopic detection of thoracic ducts after ultrasound-guided intrahepatic injection of indocyanine green detected by near-infrared fluorescence and methylene blue in dogs. Vet Surg. 2022;51(S1):O118-27. https://doi.org/10.1111/vsu.13682.
21. Morris KP, Singh A, Holt DE, Stefanovski D, Singhal S, Bosco J, et al. Hybrid single-port laparoscopic cisterna chyli ablation for the adjunct treatment of

chylothorax disease in dogs. Vet Surg. 2019;48(S1):O121-9. https://doi.org/10.1111/vsu.13195.
22. Mullen KM, Regier PJ, Perez-Rodriguez V, Fox-Alvarez WA, Bertran J, Colee J. Use of real-time near-infrared fluorescence to assess gastric viability in dogs with gastric dilatation volvulus: a case-control study. Vet Surg. 2024;53(4):684–94. https://doi.org/10.1111/vsu.14067.
23. Suh YJ, Choi JY, Chai YJ, Kwon H, Woo JW, Kim SJ, et al. Indocyanine green as a near-infrared fluorescent agent for identifying parathyroid glands during thyroid surgery in dogs. Surg Endosc. 2015;29(9):2811–7. https://doi.org/10.1007/s00464-014-3971-2.
24. Ferrari R, Chiti LE, Manfredi M, Ravasio G, De Zani D, Zani DD, et al. Biopsy of sentinel lymph nodes after injection of methylene blue and lymphoscintigraphic guidance in 30 dogs with mast cell tumors. Vet Surg. 2020;49:1099–108. https://doi.org/10.1111/vsu.13483.
25. Séguin B, Liptak JM. Updates in surgical oncology. Vet Clin North Am Small Anim Pract. 2024;54(3):577–89. https://doi.org/10.1016/j.cvsm.2023.12.010.
26. Meuten DJ, Moore FM, Donovan TA, Bertram CA, Klopfleisch R, Foster RA, et al. International guidelines for veterinary tumor pathology: a call to action. Vet Pathol. 2021;58(5):766–94. https://doi.org/10.1177/03009858211013712.
27. DE Almeida M, Gregório H, Pereira A, Queiroga FL. The diagnostic yield of Whole-body computed tomography in dogs and cats in the oncology setting. Vivo. 2025;39(3):1293–302. https://doi.org/10.21873/invivo.1393328.
28. Suami H, Yamashita S, Soto-Miranda MA, Chang DW. Lymphatic territories (lymphosomes) in a canine: an animal model for investigation of postoperative lymphatic alterations. PLoS One. 2013. https://doi.org/10.1371/journal.pone.0069222.
29. Baum H. The Lymphatic System of the Dog. Saskatoon, SK, Canada: University of Saskatchewan; 2021.
30. Worden NJ, Bertran J, Watt MM, Reynolds PS, de Mello Souza CH, Maxwell EA, et al. Superficial anatomic landmarks can be used to triangulate the location of canine peripheral lymphocentrums: superficial cervical, axillary, and superficial inguinal. J Am Vet Med Assoc. 2023;261:490–9. https://doi.org/10.2460/javma.22.11.0518.
31. Worden NJ, Bertran J, Reynolds PS, Chase EC, Crews CD, Ham K, et al. Geometric, landmark-guided technique reduces tissue trauma, surgery time, and subjective difficulty for canine peripheral lymphadenectomies: an educational crossover study. J Am Vet Med Assoc. 2023;261(11):1–9. https://doi.org/10.2460/javma.23.04.0206.
32. Verbeek FPR, Troyan SL, Mieog JSD, Liefers GJ, Moffitt LA, Rosenberg M, et al. Near-infrared fluorescence sentinel lymph node mapping in breast cancer: a multicenter experience. Breast Cancer Res Treat. 2014;143:333–42. https://doi.org/10.1007/s10549-013-2802-9.
33. Wang Y, Peng Q, Sun P, Li X, Dong Y. Comparison of Sentinel lymph node biopsy by blue dye conjunction with indocyanine green or radioisotope in early-stage breast cancer: a prospective single-center observational study. Clin Med Insights Oncol. 2023. https://doi.org/10.1177/11795549231201129.
34. Mcmasters KM, Wong SL, Chao C, Woo C, Tuttle TM, Noyes RD, et al. Defining the optimal surgeon experience for breast cancer sentinel lymph node biopsy: a model for implementation of new surgical techniques. Ann Surg. 2001. https://doi.org/10.1097/00000658-200109000-00003.
35. Lipsitz SR, Kim K, Zhao L. Analysis of repeated categorical data using generalized estimating equations. Stat Med. 1994;13(11):1149–63. https://doi.org/10.1002/sim.4780131106.
36. Shankar V, Bangdiwala SI. Observer agreement paradoxes in 2x2 tables: comparison of agreement measures. BMC Med Res Methodol. 2014. https://doi.org/10.1186/1471-2288-14-100.
37. Halekoh U, Højsgaard S, Yan J. The R Package geepack for Generalized Estimating Equations [Internet]. JSS Journal of Statistical Software. 2006. Available from: http://www
38. Stevenson MM, Marshall J, Sanchez J, Thornton R, Reiczigel J, Robison-Cox J. Title Tools for the Analysis of Epidemiological Data. 2024. Available from: https://orcid.org/0000-0003-1890-9784.
39. Kilem L. Gwet. Title Computing Chance-Corrected Agreement Coefficients (CAC). 2022. Available from: http://agreestat
40. Gariboldi EM, Stefanello D, Nolff MC, De Zani D, Zani D, Grieco V, et al. Sentinel lymph node biopsy is feasible in dogs with scars from prior local excision of solid malignancies. Animals. 2022. https://doi.org/10.3390/ani12172195.
41. Favril S, Abma E, Stock E, Devriendt N, Van Goethem B, Blasi F, et al. Fluorescence-guided surgery using indocyanine green in dogs with superficial solid tumours. Vet Rec. 2020;187:273. https://doi.org/10.1136/vr.105554.
42. Suami H, O'Neill JK, Pan WR, Taylor GI. Perforating lymph vessels in the canine torso: direct lymph pathway from skin to the deep lymphatics. Plast Reconstr Surg. 2008;121:31–6. https://doi.org/10.1097/01.prs.0000293753.93274.21.
43. Sánchez-Margallo FM, Brun MV, Sánchez-Margallo JA. Identification of intra-abdominal lymphatics in canine carcasses by laparoscopic fluorescence lymphography with intradermal and intrapopliteal ICG administration. PLoS One. 2020. https://doi.org/10.1371/journal.pone.0241992.
44. Schaafsma BE, Mieog JSD, Hutteman M, Van Der Vorst JR, Kuppen PJK, Löwik CWGM, et al. The clinical use of indocyanine green as a near-infrared fluorescent contrast agent for image-guided oncologic surgery. J Surg Oncol. 2011. https://doi.org/10.1002/jso.21943.
45. Wishart GC, Loh SW, Jones L, Benson JR. A feasibility study (ICG-10) of indocyanine green (ICG) fluorescence mapping for sentinel lymph node detection in early breast cancer. Eur J Surg Oncol. 2012;38:651–6. https://doi.org/10.1016/j.ejso.2012.05.007.
46. Cozzaglio L, Doci R, Celotti S, Roncalli M, Gennari L. Gastric cancer: extent of lymph node dissection and requirements for a correct staging. Tumori. 2004;90(5):467–72. https://doi.org/10.1177/030089160409000505.
47. Mickelson MA. Updated concepts in oncologic surgery: apocrine gland anal sac adenocarcinoma and mast cell tumors. Vet Clin North Am Small Anim Pract. 2022;52(2):549–80. https://doi.org/10.1016/j.cvsm.2021.12.008.
48. Stefanello D, Gariboldi EM, Boracchi P, Ferrari R, Ubiali A, De Zani D, et al. Weishaar's classification system for nodal metastasis in sentinel lymph nodes: clinical outcome in 94 dogs with mast cell tumor. J Vet Intern Med. 2024;38:1675–85. https://doi.org/10.1111/jvim.16997.
49. Van Den Berg NS, Brouwer OR, Klop WMC, Karakullukcu B, Zuur CL, Tan IB, et al. Concomitant radio- and fluorescence-guided sentinel lymph node biopsy in squamous cell carcinoma of the oral cavity using ICG-99mTc- nanocolloid. Eur J Nucl Med Mol Imaging. 2012;39:1128–36. https://doi.org/10.1007/s00259-012-2129-5.
50. Kuvaldina AB, Buote N, Campoy L, Porter I, Hayes GM. Development of a minimally invasive endoscopic technique for excisional biopsy of the axillary lymph nodes in dogs. Vet Surg. 2023;52:888–96. https://doi.org/10.1111/vsu.13901.
51. Tagaya N, Yamazaki R, Nakagawa A, Abe A, Hamada K, Kubota K, et al. Intraoperative identification of sentinel lymph nodes by near-infrared fluorescence imaging in patients with breast cancer. Am J Surg. 2008;195:850–3. https://doi.org/10.1016/j.amjsurg.2007.02.032.
52. Tagaya N, Nakagawa A, Abe A, Iwasaki Y, Kubota K. Non-invasive identification of sentinel lymph nodes using indocyanine green fluorescence imaging in patients with breast cancer. Open Surg Oncol J. 2010. https://doi.org/10.2174/1876504101002010071.
53. Crane LMA, Themelis G, Arts HJG, Buddingh KT, Brouwers AH, Ntziachristos V, et al. Intraoperative near-infrared fluorescence imaging for sentinel lymph node detection in vulvar cancer: first clinical results. Gynecol Oncol. 2011;120:291–5. https://doi.org/10.1016/j.ygyno.2010.10.009.
54. Brissot HN, Edery EG. Use of indirect lymphography to identify sentinel lymph node in dogs: a pilot study in 30 tumours. Vet Comp Oncol. 2017;15(3):740–53. https://doi.org/10.1111/vco.12214.
55. Goyal A, Douglas-Jones AG, Newcombe RG, Mansel RE. Effect of lymphatic tumor burden on sentinel lymph node biopsy in breast cancer. Breast J. 2005;11(3):188–94. https://doi.org/10.1111/j.1075-122X.2005.21591.x.

Publisher's Note